Brazilian Journal of Microbiology (2024) 55:143–154
https://doi.org/10.1007/s42770-023-01168-y

BIOTECHNOLOGY AND INDUSTRIAL MICROBIOLOGY - RESEARCH PAPER

Chitosan nanoparticles encapsulating farnesol evaluated in vivo against *Candida albicans*

Adelaide Fernandes Costa[1] · Jacqueline Teixeira da Silva[1] · Juliana Assis Martins[1] · Viviane Lopes Rocha[1] · Liliana Borges de Menezes[1] · Andre Correa Amaral[1]

Received: 30 August 2023 / Accepted: 26 October 2023 / Published online: 14 November 2023

Abstract

Farnesol is a natural essential oil with antimicrobial properties. Complexation of farnesol in chitosan nanoparticles can be useful to improve its bioavailability and potentiate its antifungal capabilities such as inhibition of hyphal and biofilm formation. The aim of this study was to develop and characterize chitosan nanoparticles with farnesol (NF) and evaluate their toxicity and antifungal action on *C. albicans* in vivo. The NF were prepared by the ionic gelation method and showed physicochemical characteristics such as diameter less than 200 nm, monodisperse distribution, positive zeta potential, spherical morphology, and stability after 120 days of storage. In the evaluation of toxicity in *Galleria mellonella*, NF did not reduce the survival rate, indicating that there was no toxicity in vivo at the doses tested. In the assays with *G. mellonella* infected by *C. albicans*, the larvae treated with NF had a high survival rate after 48 h, with a significant reduction of the fungal load and inhibition of the formation of biofilms and hyphae. In the murine model of vulvovaginal candidiasis (VVC), histopathological analysis showed a reduction in inflammatory parameters, fungal burden, and hyphal inhibition in mice treated with NF. The produced nanoparticles can be a promising alternative to inhibit *C. albicans* infection.

Keywords Nanotechnology · Chitosan · Farnesol · *Galleria mellonella*

Introduction

Farnesol was the first *quorum-sensing* molecule discovered in *Candida albicans*. Among its properties, the ability to inhibit the development of biofilms and the formation of hyphae stands out [1]. Despite being considered a low-risk substance, tools that reduce toxicity and improve bioavailability, such as encapsulation in nanoparticles, may be important for its wide use in antimicrobial therapies [2].

Natural polymers such as chitosan are widely used to encapsulate therapeutic agents, including farnesol [3, 4]. Chitosan nanoparticles are considered antimicrobial, mucoadhesive, biodegradable, and biocompatible [5]. The encapsulation of farnesol in chitosan nanoparticles can improve solubility, systemic absorption, bioavailability, and stability and reduce the toxicity of this molecule [6]. Also, chitosan nanoparticles with farnesol may be promising in the treatment of *C. albicans* infections due to the combined antimicrobial action of chitosan and farnesol [7].

Preclinical models using vertebrate animals have been the gold standard for in vivo testing for many years. Because of their similarities to human biological systems, they are often used to assess the toxicity and biological activities of drugs, among other aspects [8]. Mice are one of the most widely used mammalian models, but their use can be expensive and laborious and pose ethical dilemmas. Invertebrate models are promising new options for in vivo assays [9]. *Galleria mellonella* larvae have stood out as a recommended organism to verify the pathogenesis, immune responses, virulence, toxicity, and antimicrobial responses of some microorganisms such as *C. albicans* [10]. Studies with these animals indicate a good correlation both for the data observed in vitro and those results using mammalian models [11].

Determining in vivo toxicity and antifungal action in new experimental models such as *G. mellonella*, in addition to in vitro and murine tests, may be useful in evaluating the

Responsible Editor: Celia Maria de Almeida Soares

✉ Adelaide Fernandes Costa
adelaidefernandes@ufg.br

[1] Biotechnology, Institute of Tropical Pathology and Public Health, Universidade Federal de Goiás, Goiânia, GO 74605-050, Brazil

safety and efficacy of nanoparticles. In addition, in vivo antifungal tests in *G. mellonella* larvae can significantly reduce the use of mammals to evaluate drugs and molecules with therapeutic potential [12]. This work aims to develop chitosan nanoparticles containing farnesol and evaluate the antifungal activity against *C. albicans* in vivo using *G. mellonella* and in the murine model of VVC.

Materials and methods

Materials

Acetic acid (Neon, Brazil), DMSO (Hexis, Brazil), estradiol valerate (Therapeutica, Brazil), ethanol (Neon, Brazil), farnesol 95% F203 (Sigma-Aldrich, USA), formaldehyde (Neon, Brazil), methanol (Neon, Brazil), NaOH (Hexis, Brazil), low molecular weight chitosan (Sigma-Aldrich, USA), miconazole cream 2% (Teuto, Brazil), polysorbate 80 (Neon, Brazil), Sabouraud dextrose agar (HiMedia, India), sodium tripolyphosphate (Sigma-Aldrich, USA), and streptomycin (Sigma-Aldrich, USA) were utilized in this study.

Farnesol characteristics and dilution

Farnesol was commercially obtained as a light-yellow liquid solution, composed of a mixture of isomers, 95% purity, density of 0.886 g/mL at 20 °C, and molecular weight of 222.37 g/mol. For the tests, the solution was prepared by diluting farnesol in pure methanol to obtain a concentration of 444 mg/mL. A fresh farnesol solution was prepared prior to each test.

Preparation of nanoparticles

Chitosan nanoparticles with farnesol (NF) were produced by the ionic gelation technique [13]. Briefly, a chitosan solution (2 mg/mL) was prepared by dissolving the polymer in 0.1 M acetic acid by ultrasonic sonication using a Branson Sonifier 250 (level three, constant output) for 10 min. One hundred microliters of farnesol diluted in polysorbate 80 (1:1) was added to the chitosan solution and was immediately sonicated for 5 min. The pH of the solution was adjusted to 4.1 using 0.1 M NaOH. Then, 10 mL of sodium tripolyphosphate (TPP, 1 mg/mL) was added to 15 mL of the chitosan solution containing farnesol for a final concentration of 888 µg/mL. The nanoparticle's dispersion was kept under magnetic stirring for 40 min and then centrifuged three times (15 min, 13,000 rpm). The supernatants from the centrifugations were collected for quantification of farnesol, and the nanoparticles were resuspended in ultrapure water for characterization. Chitosan nanoparticles (NQ) were prepared following the same methodology but without the addition of farnesol.

Characterization of nanoparticles

The diameter and polydispersity index (PDI) were obtained by the dynamic light scattering (DLS) technique. The zeta potential values were obtained by the electrophoretic light scattering technique (Zetasizer Nano ZS, Malvern Panalytical®). The concentration of farnesol associated with the nanoparticles was determined by quantifying the farnesol (by ultraviolet spectrophotometry at 405 nm) in the nanoparticle's supernatant obtained after three successive centrifugations. The empty nanoparticle's supernatants were used as blank. Association efficiency (AE) was determined by Eq. 1:

$$\mathrm{AE}\ \% = [(\text{total farnesol} - \text{free farnesol})/\text{total farnesol}] \times 100 \quad (1)$$

The morphology of NQ and NF was evaluated by scanning electron microscopy (SEM). The JEOL JSM 7100F scanning electron microscope was used to obtain images at up to × 100,000 magnification.

Stability of nanoparticles

The stability of the nanoparticles was evaluated considering the parameters of the diameter, PDI, and zeta potential after 60, 120, and 320 days of storage at 2–8 °C.

Toxicity investigation in the *G. mellonella*

The different stages of the life cycle of *G. mellonella* were kept in the laboratory at room temperature. Ethical approval is not required for *G. mellonella* trials. In the in vivo toxicity tests, last instar larvae weighing an average of 200 mg were used. Survival rate was evaluated using $n = 10$ larvae per group. Ten microliters of the compounds diluted in phosphate-buffered saline (PBS) was injected into the last proleg of the larvae using a 10-µL Hamilton™ syringe: NQ (60 mg/kg), farnesol (710 mg/kg to 22.18 mg/kg), and NF (29.3 mg/kg). PBS 1X and DMSO P.A. were used as negative and positive controls, respectively. The larvae were kept at room temperature in Petri dishes for a period of 5 days with daily observations of mortality. After the end of the test, the surviving larvae were stored at −20 °C for later disposal.

C. albicans infection in *G. mellonella*

For the in vivo evaluation of the antifungal activity, late-stage *G. mellonella* larvae were used, with an average weight of 200 mg, infected with *C. albicans* ATCC 10231 at a concentration of 1×10^6 cells/larva. The groups ($n =$

Table 1 Characterization of chitosan nanoparticles and chitosan nanoparticles with farnesol

	NQ	NF
Diameter (nm)	147.3 ± 13.62	161.4 ± 17.71
PDI	0.238 ± 0.023	0.200 ± 0.042
Zeta potential (mV)	40.53 ± 2.49*	20.9 ± 3.37
AE (%)	N.A.	66 ± 0.51

The results express the mean ± SD ($n = 3$)

NQ chitosan nanoparticles, *NF* chitosan nanoparticles with farnesol, *N.A.* not applicable

*$p < 0.05$

10) evaluated were (i) negative control, not infected and treated with PBS; (ii) positive control, infected and treated with PBS; (iii) infected and treated with NQ (60 mg/kg); (iv) infected and treated with farnesol (29.3 mg/kg); and (v) infected and treated with NF (29.3 mg/kg). For infection, 10 µL of *C. albicans* inoculum was injected into the last right proleg of the larvae using a 0.3-unit insulin syringe (BD Ultra-Fine® II, cod:328325). After a period of 10 min, the larvae received 10 µL of the treatments in the last left proleg. The larvae were kept at 37 °C for 48 h. The survival rate was obtained from the observation of larval mortality after 24 and 48 h. At the end of the test, five larvae from each group were subjected to hemolymph collection for fungal load analysis, and another five were fixed in formaldehyde for histopathological analysis. For analysis of the fungal load, the hemolymph of *G. mellonella* was collected from a dorsal cut with a scalpel. The material obtained from each larva (10 µL) was seeded in Sabouraud agar (SA) plates that were kept at 37 °C for 48 h. After this period, the fungal load was determined by CFU counting.

For histopathological analyses, the entire larvae were fixed in 20 mL of 10% buffered formalin for 10 days. Subsequently, they were subjected to five cross-sections that resulted in six segments (two distal, two median, and two proximal). The segments of the larvae were fixed, clarified, embedded in paraffin, and submitted to a 5 µm cut with a microtome. The slides were prepared and stained with hematoxylin and eosin (HE) and periodic acid–Schiff (PAS).

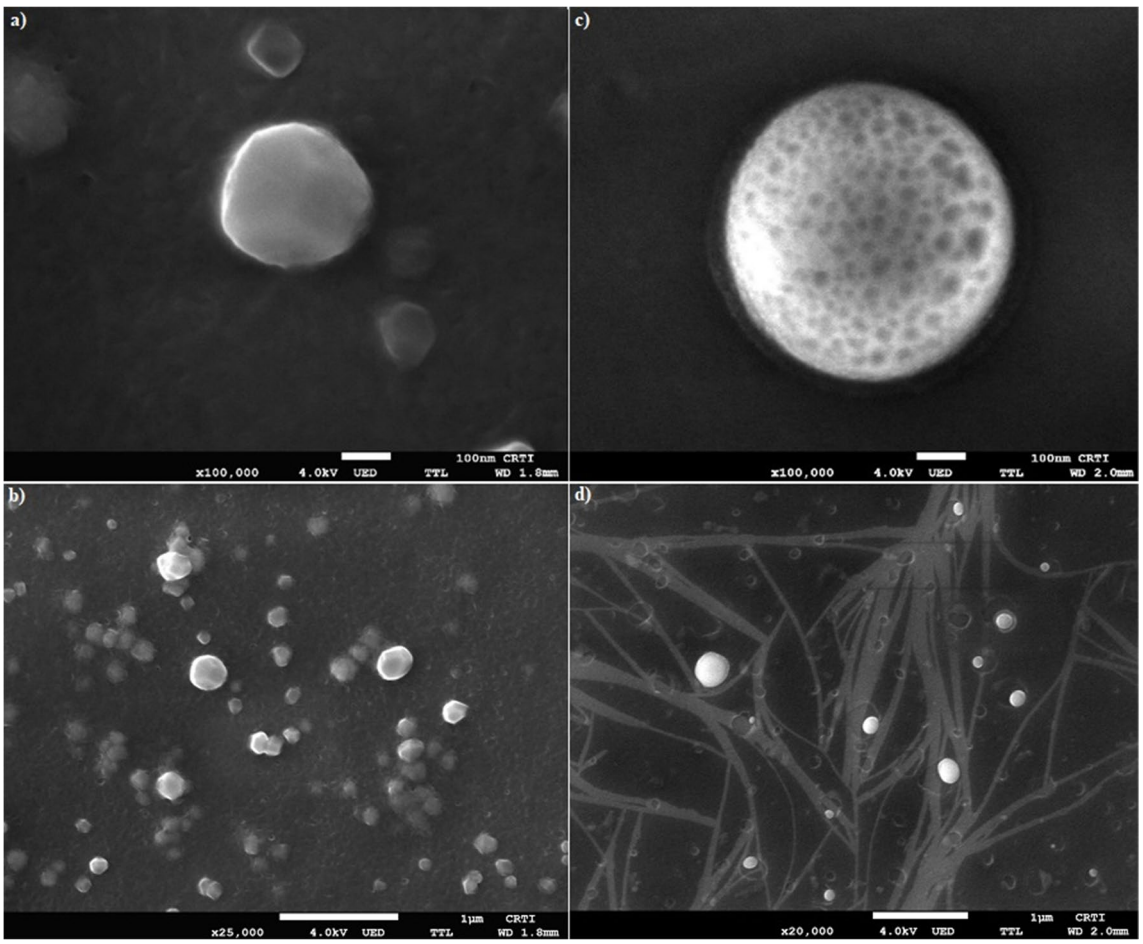

Fig. 1 Images obtained by scanning electronic microscopy with magnification of up to × 100,000. Chitosan nanoparticles (**a**, **b**); chitosan nanoparticles with farnesol (**c**, **d**)

Table 2 Stability of nanoparticles during 320 days

Parameters	Time (days)			
	0	60	120	320
NQ				
Diameter (nm)	147.3 ± 13.62	174.7 ± 9.50*	209.8 ± 18.52*	197.9 ± 11.27*
PDI	0.238 ± 0.023	0.334 ± 0.028*	0.34 ± 0.025*	0.351 ± 0.014*
Zeta potential (mV)	+40.53 ± 2.49	+38.6 ± 3.94	+35.7 ± 2.79	+32.4 ± 2.53*
NF				
Diameter (nm)	161.4 ± 17.71	254 ± 13.50*	240.6 ± 10.08*	276.5 ± 15.20*
PDI	0.200 ± 0.042	0.412 ± 0.031*	0.457 ± 0.024*	0.476 ± 0.036*
Zeta potential (mV)	+20.9 ±3.37	+20.7 ± 14.3	+29.7 ± 12.7	+28.0 ±2.19*

The results express the mean ± SD ($n = 3$)

NQ chitosan nanoparticles, *NF* chitosan nanoparticles with farnesol, *PDI* polydispersity index

*$p < 0.05$

The tissues were observed under an optical microscope at magnifications of ×40, ×100, and ×400. A semiquantitative analysis was carried out based on the count of fungal clusters of *C. albicans* present in different fragments of the larvae. The infection was considered severe when the count was above 30, moderate between 10 and 29, mild from 1 to 9, and absent when there was no formation of fungal clusters in the tissues.

Murine model of VVC

The use of animals for experimentation was approved by the Ethics Committee for the Use of Animals of the Federal University of Goiás (UFG). Eight- to 10-week-old female BALB/c mice were obtained and maintained in the Center for Animal Production and Experimentation at UFG under controlled light conditions, with free access to water and a standard diet for the species.

The mice received a subcutaneous dose of 100 µL of estradiol valerate diluted in castor oil (0.3 mg/mL). This procedure was performed 3 days before infection and repeated weekly to induce a pseudo-estrus state and a persistent vaginal infection in the mouse. The *C. albicans* fungus cells were resuspended in PBS and counted to obtain a concentration of 7.5×10^7 yeasts/mL. Infection was performed by inoculating 20 µL of the yeast suspension vaginally using a mechanical micropipette. The mice were divided into five groups ($n = 5$): (i) negative control, not infected and treated with PBS; (ii) positive control, infected and treated with PBS; (iii) infected and treated with 2% miconazole cream (50 mg/kg); (iv) infected and treated with NQ (60 mg/kg); and (v) infected and treated with NF (29.3 mg/kg). After 48 h of infection, 20 µL of the different treatments was administered

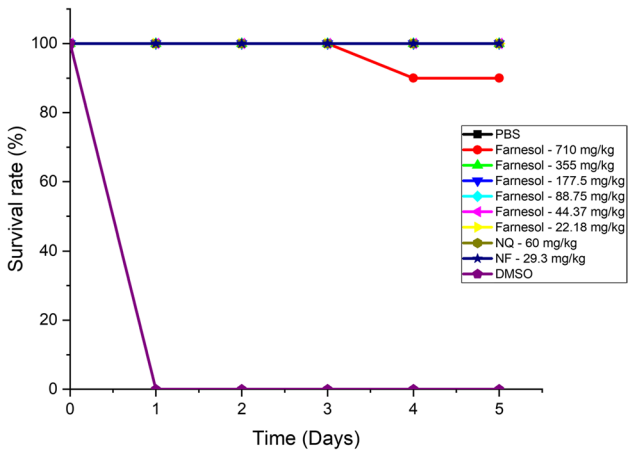

Fig. 2 Survival rate of *Galleria mellonella* after treatments with farnesol (22.18 to 710 mg/kg), NQ (chitosan nanoparticles 60 mg/kg) and NF (chitosan nanoparticles with farnesol 29.3 mg/kg) for 5 days

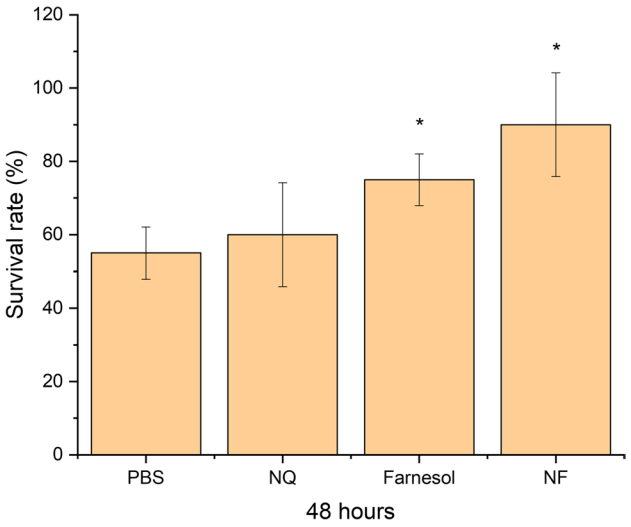

Fig. 3 Survival rate after 48 h of *Galleria mellonella* larvae infected by *Candida albicans* ATCC 10231 and treated with PBS (phosphate-buffered saline 1X), NQ (chitosan nanoparticles 60 mg/kg), farnesol (29.3 mg/kg), and NF (chitosan nanoparticles with farnesol 29.3 mg/kg). ($p < 0.05$)*

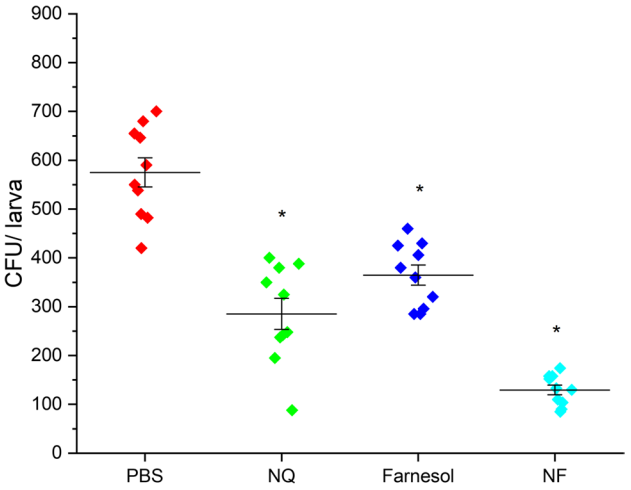

Fig. 4 CFU/larva obtained from *Galleria mellonella* infected with *Candida albicans* ATCC 10231 and treated with PBS (phosphate-buffered saline 1X), NQ (chitosan nanoparticles 60 mg/kg), farnesol (29.3 mg/kg), and NF (chitosan nanoparticles with farnesol 29.3 mg/kg). ($p < 0.05$)*

vaginally, once a day, for 7 consecutive days. Twenty-four hours after the end of treatment, the animals were euthanized by cervical dislocation. In a biological safety cabinet, vaginal tissues were extracted and cut longitudinally for fungal load and histopathological analysis. Fungal load recovery was performed by macerating the vaginal tissue in 1 mL of PBS. The total volume was divided into three SA plates (containing 10 µg/mL of streptomycin) and kept at 37 °C for 48 h. The results were obtained from the CFU count per gram of vaginal tissue of the animals.

For histopathological analysis, longitudinal sections of the vaginal tissues were fixed, clarified, embedded in paraffin, and sectioned with a microtome. The slides were prepared and stained with HE and PAS. Analyses were performed by optical microscopy in 10 fields at ×100 and ×400 magnifications, according to the following criteria for classification of inflammation: (1) absent (absence of neutrophils), (2) mild inflammation (one to ten neutrophils or one to three microabscesses in the epithelial layer and a few neutrophils in the submucosa), (3) moderate inflammation (between 11 and 20 neutrophils or four to six microabscesses in the epithelial layer and a few neutrophils in the submucosa), and (4) marked inflammation (> 20 neutrophils or > 6 microabscesses and a few neutrophils in the submucosa). With PAS staining, the presence, absence, and morphology of *C. albicans* in the lumen or vaginal epithelium were evaluated.

Statistical analysis

Results were expressed as mean ± standard deviation (SD). Statistical analyses were performed by *t*-student test and analysis of variance (ANOVA) with Tukey's post hoc test ($p < 0.05$)* in the Origin 2018 software.

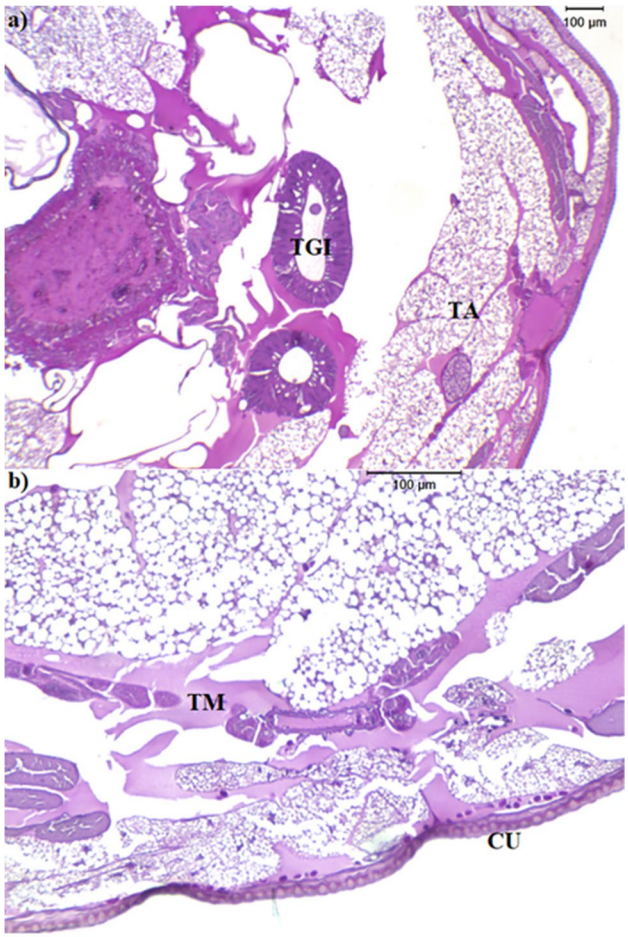

Fig. 5 Photomicrograph of *Galleria mellonella* larvae stained with periodic acid–Schiff: **a**, **b** uninfected and treated with PBS (phosphate-buffered saline 1X). ×40X and ×100 magnifications. TGI gastrointestinal tract, TM muscle tissue, TA adipose tissue, CU cuticle

Results

Characterization of nanoparticles

The NQ and NF presented mean diameters of 147.3 ± 10.40 nm and 161.4 ± 13.31 nm, respectively, and were considered monodisperse with mean PDI values less than 0.250. The zeta potential was positive, and it was higher for NQ ($p < 0.05$). Considering the AE of 66%, approximately 586 µg/mL of farnesol was encapsulated in the nanoparticles (Table 1).

The images obtained by SEM of NQ and NF demonstrated the spherical morphology of the nanostructures (Fig. 1). The similar morphologies indicated that there was

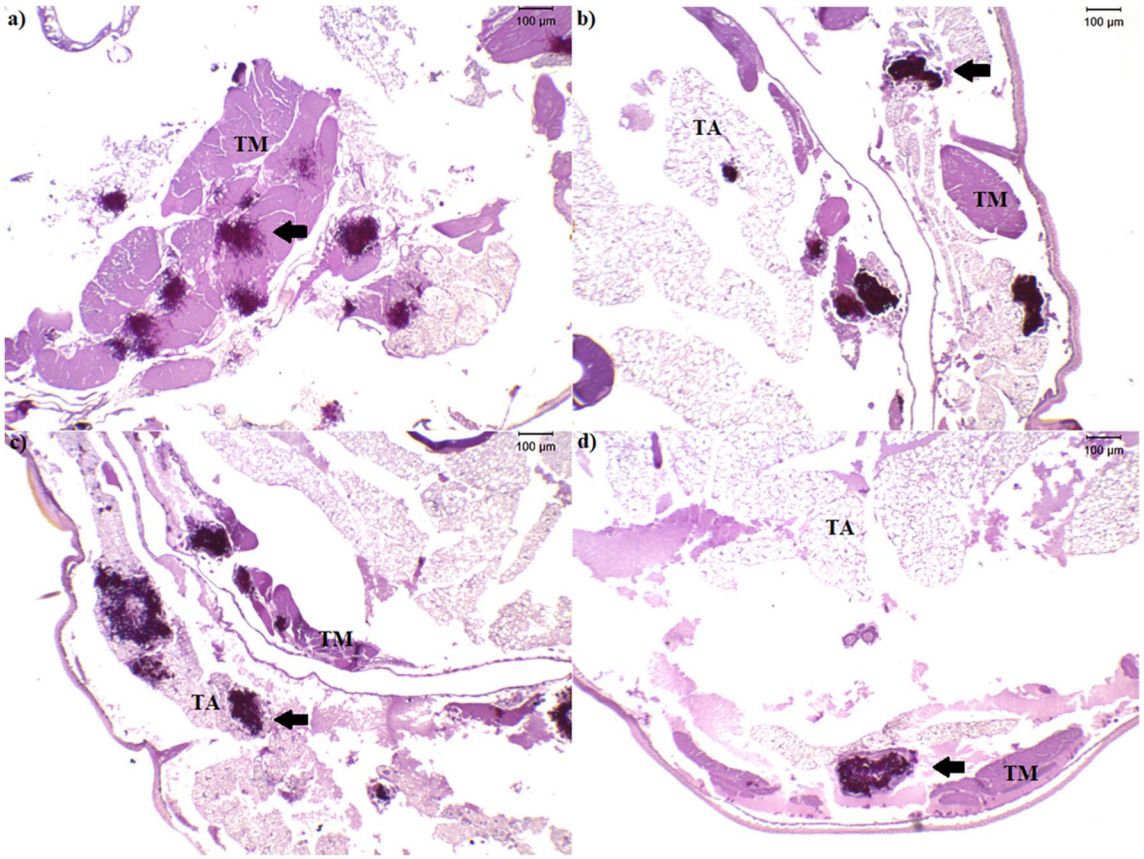

Fig. 6 Photomicrograph of *Galleria mellonella* larvae infected with *Candida albicans* and stained with periodic acid–Schiff: **a** infected and treated with PBS (phosphate-buffered saline 1X); **b** infected and treated with chitosan nanoparticles; **c** infected and treated with farnesol; **d** infected and treated with chitosan nanoparticles with farnesol. ×40 magnification. TM muscle tissue, TA adipose tissue; black arrow denotes presence of fungi

no change in this parameter with the encapsulation of the molecule. The methodology visually confirmed the formation of particles at the nanometer scale.

Stability investigation of nanoparticles

The results of the NQ and NF stability evaluation showed a statistically significant increase in diameter and PDI after 60, 120, and 320 days ($p < 0.05$) (Table 2). After 320 days, NQ presented a reduction in zeta potential, while an increase was observed for NF when compared to time 0 ($p < 0.05$). Despite parameter variations during the evaluated period, NQ and NF remained at the nanometer scale, monodisperse, and with a positive zeta potential after the long storage period, which indicates the stability of the preparation.

Toxicity to *G. mellonella*

The toxicity of farnesol and nanoparticles was determined in the in vivo model of *G. mellonella* larvae (Fig. 2). The larvae that received farnesol at doses between 22.18 and 355 mg/kg had a 100% survival rate during the 5 days evaluated. The dose of 710 mg/kg reduced survival to 90% after the fourth day. The administration of NQ and NF did not reduce the survival rate of the larvae, which remained at 100% during the 5 days. The high survival rates characterize farnesol, NQ, and NF as non-toxic in vivo at the doses tested.

C. albicans infection in *G. mellonella*

In the infection test of *G. mellonella* larvae with *C. albicans* and treatment with the different formulations, it was observed that the survival rate of the larvae after 24 h was 100% for all groups. In the evaluation of 48 h, the uninfected group treated with PBS remained with 100% survival. Meanwhile, those infected with *C. albicans* and treated with PBS had a survival rate of 55 ± 7.07%. Treatments with NQ and farnesol increased the larval survival rate to 60 ± 14.14% and 75 ± 7.07%, respectively. The larvae treated with NF presented 90 ± 14.14% survival, thus significantly inhibiting the mortality caused by the fungus ($p < 0.05$) in relation to the infected group treated with PBS (Fig. 3).

The CFU/larva count showed the ability of NQ, farnesol, and NF to reduce the fungal load in relation to larvae treated with PBS ($p < 0.05$). There was no statistically significant difference between NQ and farnesol results ($p > 0.05$). However, NF showed a significant reduction in the fungal load in vivo in *G. mellonella*, compared to the other treatments ($p < 0.05$) (Fig. 4).

Histopathological analyses of *G. mellonella* larvae allowed the observation of non-infected tissues treated with PBS (Fig. 5). The morphologies of adipose and muscular tissues, gastrointestinal tract, and cuticle were observed. In the tissues of the larvae infected with *C. albicans* and treated with the compounds, the presence of fungal cells that formed clusters in different tissue regions was observed (Fig. 6). According to the semiquantitative evaluation, infection was considered severe in larvae infected with *C. albicans* and treated with PBS. There was severe damage to tissue integrity, numerous fungal clusters, a high presence of hyphae, and significant invasion of adipose and muscle tissues. Treatments with farnesol and NQ showed moderate infection, evidenced by the partial reduction of tissue damage, inhibition of the amount and density of fungal clusters, and presence of hyphae. The larvae treated with NF had an infection classified as mild, with a significant reduction in the presence of hyphae and fungal clusters (Fig. 7). Additionally, treatment with NF significantly reduced the spread of the fungus in tissues. The presence of myelinated nodules was observed, evidenced by granuloma-like structures, with significant infiltrates of hemocytes around the fungal clusters. This larval immune response was not observed in larvae treated with PBS (Fig. 8).

Murine model of VVC

Antifungal activity was evaluated in the murine model for VVC. The CFU count per gram obtained from the vaginal tissues of mice infected with *C. albicans* ATCC 10231 showed that the infected animals treated with PBS had a vaginal infection with a high fungal burden. The treatment with commercial antifungal miconazole 2% (50 mg/kg) was effective in reducing the fungal load, with values close to zero. The treatments with NQ and NF were not statistically different from the positive control ($p > 0.05$), but some mice of these groups presented smaller individual

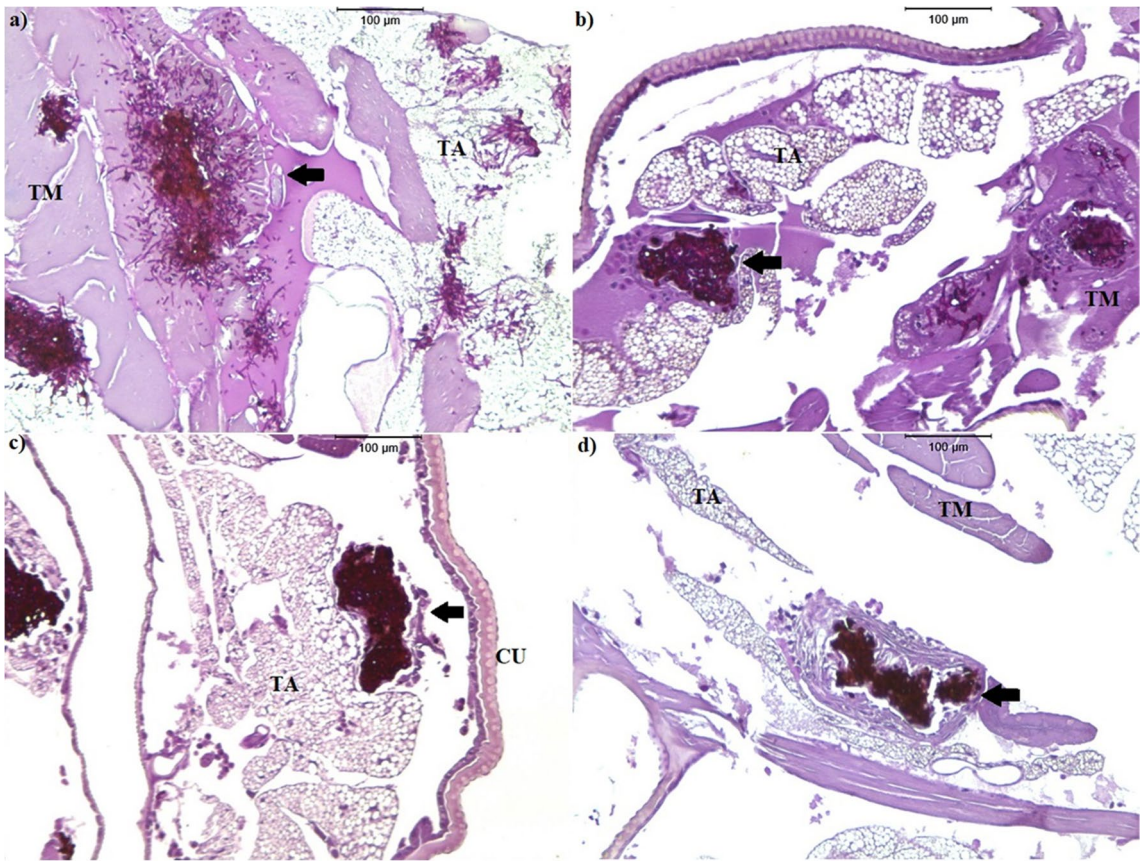

Fig. 7 Photomicrograph of *Galleria mellonella* larvae infected with *Candida albicans* and stained with periodic acid–Schiff: **a** infected and treated with PBS (phosphate-buffered saline 1X); **b** infected and treated with chitosan nanoparticles; **c** infected and treated with farnesol; **d** infected and treated with chitosan nanoparticles with farnesol. ×100 magnification. TM muscle tissue, TA adipose tissue, CU cuticle; black arrow denotes presence of fungi

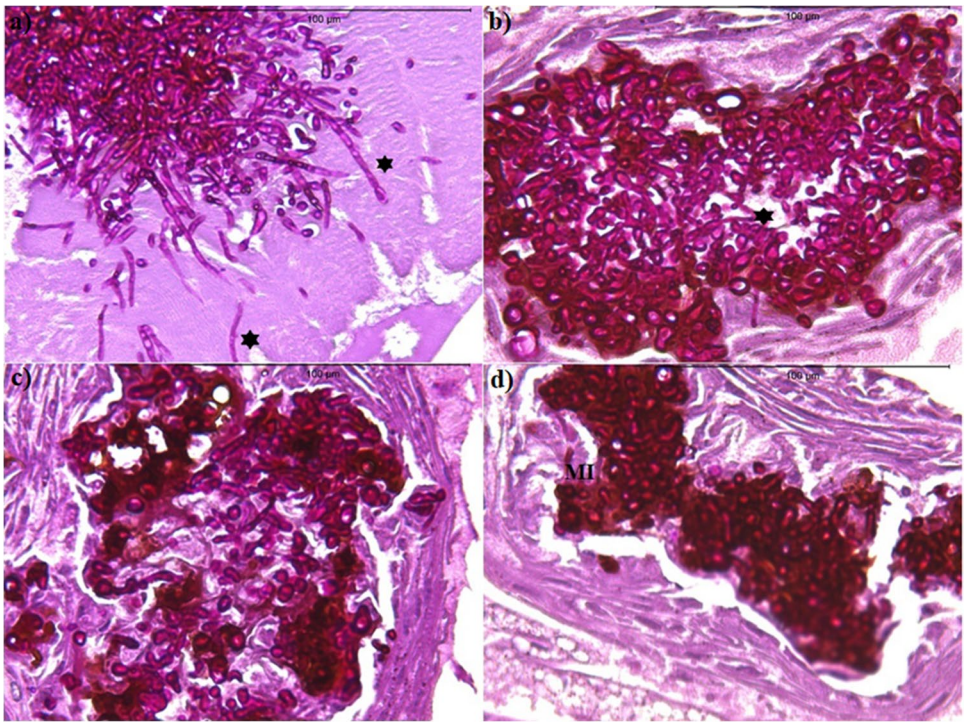

Fig. 8 Photomicrograph of *Galleria mellonella* larvae infected with *Candida albicans* and stained with periodic acid–Schiff: **a** infected and treated with PBS (phosphate-buffered saline 1X); **b** infected and treated with chitosan nanoparticles; **c** infected and treated with farnesol; **d** infected and treated with chitosan nanoparticles with farnesol. ×400 magnification. MI melanization; asterisk denotes hyphae

fungal loads. In addition, there is a gradual decrease in the mean CFU count per gram with the NQ and NF treatments; however, NF presented the lowest mean (Fig. 9).

Histopathological analyses indicated that non-infected mice treated with PBS and infected mice treated with 2% miconazole did not show significant histopathological changes, and only hyperplasia caused by the administration of estradiol valerate and inflammation was considered absent. The absence of fungal elements in the group treated with miconazole corroborates the effectiveness of treatment with the commercial antifungal. Mice infected and treated with PBS showed marked inflammation with hyperplasia, accentuated hyperkeratosis, microabscesses, and the presence of fungi in the lumen and stratum corneum, which confirms the establishment of vaginal infection in the in vivo model. Treatments with NQ and NF showed moderate inflammation, hyperplasia, moderate hyperkeratosis, and reduction of microabscesses when compared to those infected and treated with PBS (Fig. 10).

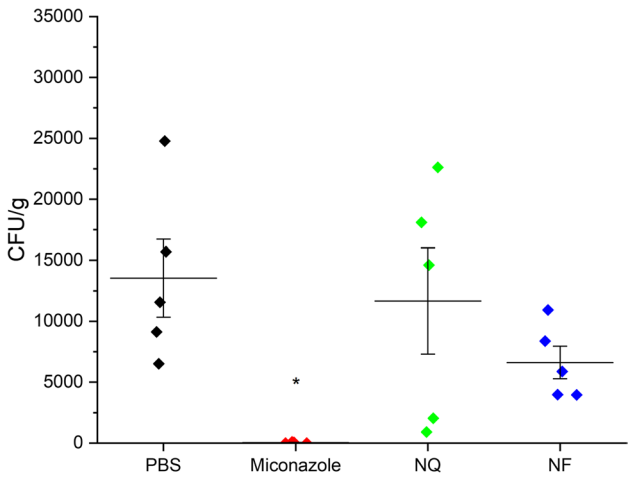

Fig. 9 CFU/g obtained from vaginal tissues treated with PBS (phosphate-buffered saline 1X), 2% miconazole (50 mg/kg), NQ (chitosan nanoparticles 60 mg/kg), and NF (chitosan nanoparticles with farnesol 29.3 mg/kg) in the murine model of vulvovaginal candidiasis

Staining with PAS allowed to observe the different morphologies of *C. albicans* in the tissue and indicated that, compared to the positive control, treatments with NQ and NF inhibited the formation of hyphae (Fig. 11). In addition, animals treated with NF showed mild inflammation and lower intensity of fungal elements.

Discussion

Farnesol is a bioactive compound with important antimicrobial properties against various fungi and bacteria [14]. The encapsulation of this molecule, which is considered a volatile essential oil, in nanometric particles can protect it from degrading environmental factors, in addition to increasing its absorption and bioefficacy [15]. Combined with the antimicrobial and mucoadhesive characteristics of chitosan [16], the developed nanoparticles may favor the use of farnesol in the treatment of microbial infections of the mucous membranes.

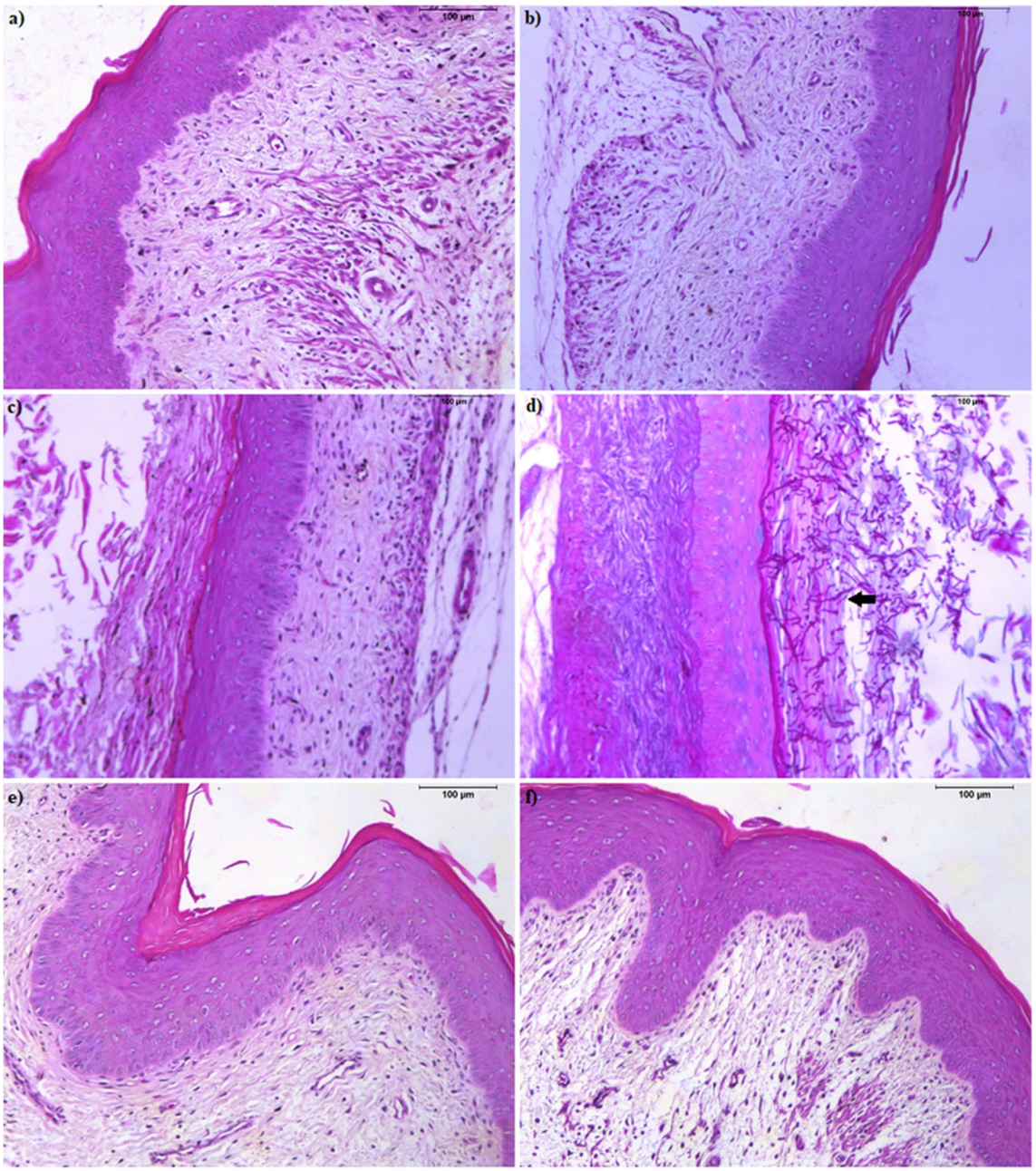

Fig. 10 Histopathological images obtained from vaginal tissue: **a** not infected and treated with PBS—HE hyperplasia; **b** infected and treated with miconazole 2%—HE hyperplasia; **c** infected and treated with PBS—HE hyperplasia, marked hyperkeratosis, microabscesses; **d** infected and treated with PBS—PAS presence of fungi in the lumen and stratum corneum (black arrow); **e** infected and treated with chitosan nanoparticles—HE hyperplasia, moderate hyperkeratosis, absence of microabscesses; **f** infected and treated with chitosan nanoparticles with farnesol—HE hyperplasia, moderate hyperkeratosis, absence of microabscesses. HE hematoxylin-eosin, PAS periodic acid–Schiff, PBS phosphate-buffered saline 1X. × 100 magnification

The NF produced presented diameter in nanometric scale, monodispersion, positive zeta potential, high AE, and good stability after 320 days, satisfactory parameters for the use of nanoparticles [17, 18]. The stability of the nanoparticles is related to the values of diameter and PDI. Values below 0.5 are considered satisfactory for the PDI, since they indicate monodispersion and homogeneity in the distribution of the nanoparticle's diameter. In addition, the increase in the values of this parameter may indicate the aggregation of nanoparticles [19]. High zeta potential values are desirable as the high particle charge can improve stability and avoid aggregation due to electrical repulsions between the

nanoparticles [20]. The zeta potential values obtained are considered favorable for stability and attachment to negatively charged mucosa, a relevant characteristic of chitosan for in vivo use, mainly for VVC application [21].

NQ and NF images by SEM demonstrated spherical morphologies and visually confirmed the formation of particles at the nanoscale. Chitosan nanogels with farnesol also presented spherical morphology, with a diameter between 43.5 and 54.6 nm and an AE of 88% [7]. Chitosan nanoparticles with eugenol, another essential oil extracted from plants, presented a diameter between 80 and 100 nm, spherical morphology, and zeta potential between + 16.23 and + 33.5 mV [22].

Size, surface charge, and morphology are usually the factors that most influence the toxicity of nanoparticles, in addition to their chemical composition [23]. Although in vitro tests provide important information regarding the biological activity of the compounds tested, it is essential to also assess in vivo toxicity. The test in larvae of *G. mellonella* stands out for allowing the determination of toxicity of several compounds efficiently, simply, and quickly when compared to models using more complex animals [10, 12]. In *G. mellonella*, the dose of 710 mg/kg of farnesol reduced survival to 90% on the fourth day, but doses below 355 mg/kg showed 100% survival. In toxicological evaluations, farnesol presented an oral LD_{50} in rats at 6000 mg/kg and in mice at 7400 mg/kg. When administered intraperitoneally to mice, LD_{50} was 443 mg/kg [24]. Data show that oral tolerance to farnesol may be higher. Another study also considered farnesol (44.4 µg/mL) non-toxic in *G. mellonella* larvae; the treatment caused one death in a group of 12 larvae [25]. NQ and NF were also not toxic to the larvae, with a 100% survival rate. In other analyses, chitosan (200 mg/kg) and chitosan nanoparticles were considered non-toxic, as they did not cause significant reductions in the survival rate in this in vivo model [26, 27].

The ability of farnesol to inhibit virulence factors, such as hyphal and biofilm formation, has received important attention, since the pathogen may have its pathogenicity reduced [28]. This therapy may be beneficial in immunocompromised patients or with recurrent infections by *C. albicans* [29, 30].

In vivo evaluation is essential to verify the activity of nanoparticles under more complex conditions, because in vitro tests cannot mimic important characteristics such as fluid flow, host proteins, and especially the influence of the immune system [31].

In the tests with *G. mellonella*, the larvae infected by *C. albicans* and treated with NF had a high survival rate after 48 h, showed reduced fungal load, and developed hyphae

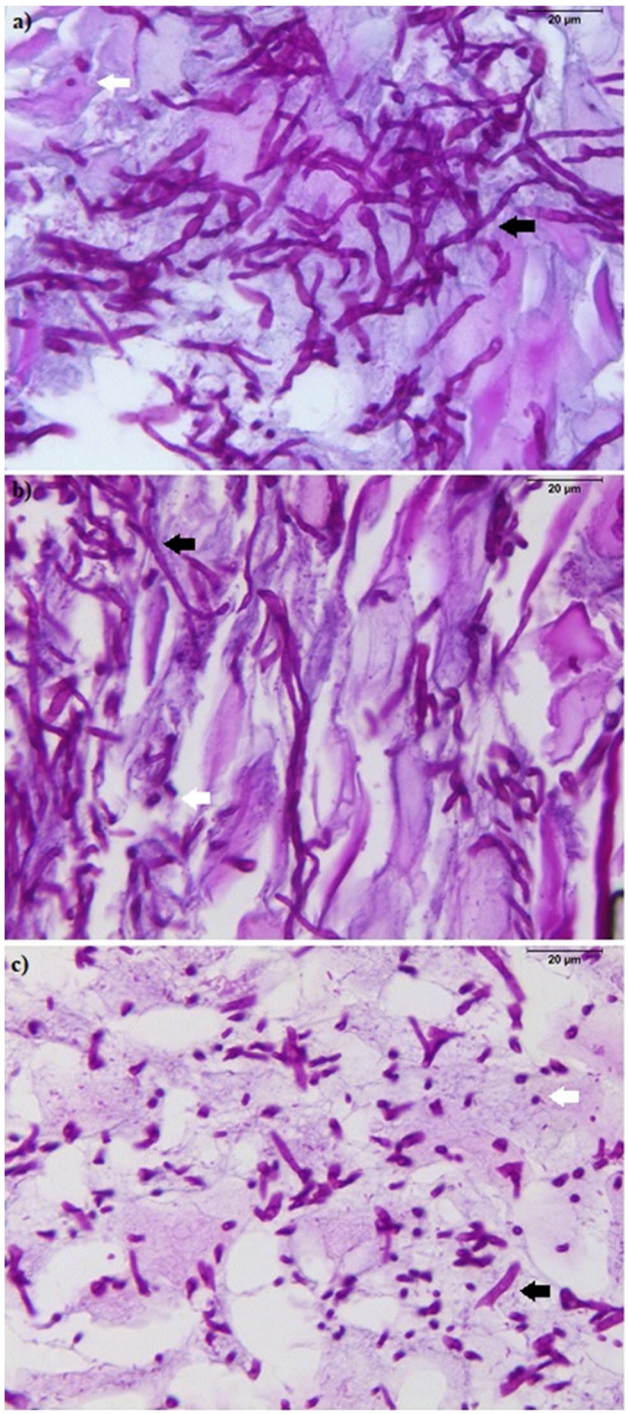

Fig. 11 Histopathological images obtained from vaginal tissue stained with PAS to observe the morphologies of *Candida albicans*: **a** infected and treated with PBS—intense presence of hyphae (black arrow) and some yeasts (white arrow); **b** infected and treated with chitosan nanoparticles—intense presence of hyphae (black arrow) and some yeasts (white arrow); **c** infected and treated with chitosan nanoparticles with farnesol—hyphal inhibition and yeast prevalence. PAS periodic acid–Schiff, PBS phosphate-buffered saline 1X. ×400 magnification

and biofilms in the tissues. The results of this in vivo model suggest the potentiation of the properties of farnesol with encapsulation in chitosan nanoparticles. It is believed that the treatments may have reduced the pathogenicity of *C. albicans* and improved the immune response, allowing to observe important defense mechanisms in *G. mellonella*, such as nodulation and melanization. In another evaluation, the treatment of *C. albicans* ATCC 90028 with farnesol (300 µM–66 µg/mL) before infection in *G. mellonella* significantly increased larval survival (77.78%) and caused a decrease in melanization when compared to the infected group without previous treatment with farnesol. Hyphal inhibition was also observed in the histopathological analysis of the larvae. With in vitro molecular analysis, the activation of apoptotic pathways by farnesol was detected, observed by increased expression of genes related to in vitro apoptosis (Card-9 and Noxa). Therefore, the apoptosis induction is related to a decrease in the pathogenicity of the fungus [32].

Larvae treated with NQ also had a higher survival rate than the positive control and reduced fungal burden. In *G. mellonella* infected with *C. auris* and treated with 200 mg/kg of chitosan, the results were similar to this work, as the polymer was not toxic for the larva, reduced the fungal load, and increased the survival rate by 55 to 84% [26].

In vivo analyses were also performed in a murine model of *C. albicans* infection. From the results of the CFU count per gram of the different treatments administered, it was observed that the treatments with NQ and NF did not present statistical differences in relation to the positive control, due to the high variation of fungal infection among positive control mice. The CFU counting method may not be appropriate for evaluating biofilms, as these consist of multicellular organisms such as hyphae, surrounded by ECM, and which can be counted as a single growing colony [33].

Histopathological analyses indicated that NF reduced the presence of hyphae in relation to positive control and treatment with NQ, again signaling its possible action in reducing virulence. In a murine model of oral candidiasis, histopathological analysis of the lingual tissues demonstrated that farnesol inhibited the presence of hyphae and reduced inflammation [34]. In the murine model of VVC, the reduction of inflammation in animals treated with chitosan nanoparticles containing farnesol was observed [4]. The results of the murine model are considered compatible with those observed in human hosts [35, 36] and showed a good correlation with the results found in *G. mellonella* larvae infected with *C. albicans*.

The results obtained in vivo corroborate the hypothesis that chitosan nanoparticles with farnesol act on *C. albicans* as an efficient inhibitor of virulence factors. Therefore, its use can reduce the invasive and pathogenic capacity of the fungus.

Funding This work was supported by the Federal University of Goiás (UFG) and the Research Support Foundation of the State of Goiás (FAPEG).

Data availability All data generated or analyzed during this study are included in this published article. The authors alone are responsible for the content and the writing of the paper.

Declarations

Competing interests The authors declare no competing interest.

References

1. Ramage G, Saville SP, Wickes BL, López-Ribot JL (2002) Inhibition of *Candida albicans* biofilm formation by farnesol, a *quorum-sensing* molecule. Appl Environ Microbiol 68(11):5459–5463. https://doi.org/10.1128/AEM.68.11.5459-5463.2002
2. Patra JK, Das G, Fraceto LF et al (2018) Nano based drug delivery systems: recent developments and future prospects. J Nanobiotechnology 16(1):71. https://doi.org/10.1186/s12951-018-0392-8
3. Arya N, Chakraborty S, Dube N, Katti DS (2009) Electrospraying: a facile technique for synthesis of chitosan-based micro/nanospheres for drug delivery applications. J Biomed Mater Res B Appl Biomater 88(1):17–31. https://doi.org/10.1002/jbm.b.31085
4. Fernandes Costa A, Evangelista Araujo D, Santos Cabral M et al (2019) Development, characterization, and *in vitro-in vivo* evaluation of polymeric nanoparticles containing miconazole and farnesol for treatment of vulvovaginal candidiasis. Med Mycol 57(1):52–62. https://doi.org/10.1093/mmy/myx155
5. Dhawan S, Singla AK, Sinha VR (2004) Evaluation of mucoadhesive properties of chitosan microspheres prepared by different methods. AAPS PharmSciTech 5(4):e67. Published 2004 Jul 26. https://doi.org/10.1208/pt050467
6. Agnihotri SA, Mallikarjuna NN, Aminabhavi TM (2004) Recent advances on chitosan-based micro- and nanoparticles in drug delivery. J Control Release 100(1):5–28. https://doi.org/10.1016/j.jconrel.2004.08.010
7. Nikoomanesh F, Roudbarmohammadi S, Khoobi M, Haghighi F, Roudbary M (2019) Design and synthesis of mucoadhesive nanogel containing farnesol: investigation of the effect on HWP1, SAP6 and Rim101 genes expression of *Candida albicans in vitro*. Artif Cells Nanomed Biotechnol 47(1):64–72. https://doi.org/10.1080/21691401.2018.1543193
8. Clark RE, Squire LR (2010) An animal model of recognition memory and medial temporal lobe amnesia: history and current issues. Neuropsychologia 48(8):2234–2244. https://doi.org/10.1016/j.neuropsychologia.2010.02.004
9. Mikulak E, Gliniewicz A, Przygodzka M, Solecka J (2018) Galleria mellonella L. as model organism used in biomedical and other studies. Przegl Epidemiol 72(1):57–73
10 Champion OL, Wagley S, Titball RW (2016) *Galleria mellonella* as a model host for microbiological and toxin research. Virulence 7(7):840–845. https://doi.org/10.1080/21505594.2016.1203486
11 Jemel S, Guillot J, Kallel K, Botterel F, Dannaoui E (2020) *Galleria mellonella* for the evaluation of antifungal efficacy against medically important fungi, a narrative review. Microorganisms 8(3):390. https://doi.org/10.3390/microorganisms8030390
12. Allegra E, Titball RW, Carter J, Champion OL (2018) *Galleria mellonella* larvae allow the discrimination of toxic and non-toxic chemicals. Chemosphere 198:469–472. https://doi.org/10.1016/j.chemosphere.2018.01.175

13. Calvo P, Remunán-López C, Vila-Jato JL (1997) Novel hydrophilic chitosan polyethylene oxide nanoparticles as protein carriers. J Appl Polym Sci 63:125–132
14 Costa AF, Silva LDC, Amaral AC (2021) Farnesol: An approach on biofilms and nanotechnology. Med Mycol 59(10):958–969. https://doi.org/10.1093/mmy/myab020
15. Bilia AR, Guccione C, Isacchi B, Righeschi C, Firenzuoli F, Bergonzi MC (2014) Essential oils loaded in nanosystems: a developing strategy for a successful therapeutic approach [retracted in: Evid Based Complement Alternat Med. 2021 Feb 15;2021:7259208]. Evid Based Complement Alternat Med 2014:651593. https://doi.org/10.1155/2014/651593
16 Abd El-Hack ME, El-Saadony MT, Shafi ME et al (2020) Antimicrobial and antioxidant properties of chitosan and its derivatives and their applications: a review. Int J Biol Macromol 164:2726–2744. https://doi.org/10.1016/j.ijbiomac.2020.08.153
17. Lai SK, Wang YY, Hida K, Cone R, Hanes J (2011) Nanoparticles reveal that human cervicovaginal mucus is riddled with pores larger than viruses [published correction appears in Proc Natl Acad Sci U S A 108(34):14371]. Proc Natl Acad Sci U S A 107(2):598-603.https://doi.org/10.1073/pnas.0911748107
18. Vaghasiya K, Sharma A, Ray E, Adlakha S, Verma RK (2020) Methods to characterize nanoparticles for mucosal drug delivery. In: Muttil P., Kunda N. (eds) Mucosal delivery of drugs and biologics in nanoparticles. AAPS Advances in the Pharmaceutical Sciences Series 41:27-57
19. Danaei M, Dehghankhold M, Ataei S, et al (2018) Impact of particle size and polydispersity index on the clinical applications of lipidic nanocarrier systems. Pharmaceutics 10(2):57. Published 2018 May 18. https://doi.org/10.3390/pharmaceutics10020057
20. Freitas C, Muller RH (1998) Effect of light and temperature on zeta potential and physical stability in solid lipid nanoparticle (SLN (TM)) dispersions. Int J Pharm 168(2):221–229. https://doi.org/10.1016/S0378-5173(98)00092-1
21. Islam MA, Park TE, Reesor E et al (2015) Mucoadhesive chitosan derivatives as novel drug carriers. Curr Pharm Des 21(29):4285–4309. https://doi.org/10.2174/1381612821666150901103819
22 Woranuch S, Yoksan R (2013) Eugenol-loaded chitosan nanoparticles: I Thermal stability improvement of eugenol through encapsulation. Carbohydr Polym 96(2):578–585. https://doi.org/10.1016/j.carbpol.2012.08.117
23. Du J, Wang S, You H, Zhao X (2013) Understanding the toxicity of carbon nanotubes in the environment is crucial to the control of nanomaterials in producing and processing and the assessment of health risk for human: a review. Environ Toxicol Pharmacol 36(2):451–462. https://doi.org/10.1016/j.etap.2013.05.007
24. National Center for Biotechnology Information (2022) PubChem Database. Farnesol, CID=3327. https://pubchem.ncbi.nlm.nih.gov/compound/Farnesol (accessed 15 May 2022).
25. Černáková L, Jordao L, Bujdáková H (2018) Impact of farnesol and Corsodyl® on *Candida albicans* forming dual biofilm with *Streptococcus mutans*. Oral Dis 24(6):1126–1131. https://doi.org/10.1111/odi.12873
26. Arias LS, Butcher MC, Short B, et al (2020) Chitosan ameliorates *Candida auris* virulence in a *Galleria mellonella* infection model [published correction appears in Antimicrob Agents Chemother. 2021 Feb 17;65(3):]. Antimicrob Agents Chemother 2020;64(8):e00476-20. https://doi.org/10.1128/AAC.00476-20
27. Cé R, Silva RC, Trentin DS et al (2020) *Galleria mellonella* larvae as an *In Vivo* model to evaluate the toxicity of polymeric nanocapsules. J Nanosci Nanotechnol 20(3):1486–1494. https://doi.org/10.1166/jnn.2020.17170
28. Pierce CG, Srinivasan A, Ramasubramanian AK, López-Ribot JL (2015) From biology to drug development: new approaches to combat the threat of fungal biofilms. Microbiol Spectr 3(3):https://doi.org/10.1128/microbiolspec.MB-0007-2014
29. Hornby JM, Jensen EC, Lisec AD et al (2001) *Quorum sensing* in the dimorphic fungus *Candida albicans* is mediated by farnesol. Appl Environ Microbiol 67(7):2982–2992. https://doi.org/10.1128/AEM.67.7.2982-2992.2001
30 Vila T, Romo JA, Pierce CG, McHardy SF, Saville SP, Lopez-Ribot JL (2017) Targeting *Candida albicans* filamentation for antifungal drug development. Virulence 8(2):150–158. https://doi.org/10.1080/21505594.2016.1197444
31 Samaranayake YH, Samaranayake LP (2001) Experimental oral candidiasis in animal models. Clin Microbiol Rev 14(2):398–429. https://doi.org/10.1128/CMR.14.2.398-429.2001
32 Singkum P, Muangkaew W, Suwanmanee S, Pumeesat P, Wongsuk T, Luplertlop N (2020) Suppression of the pathogenicity of *Candida albicans* by the *quorum-sensing* molecules farnesol and tryptophol. J Gen Appl Microbiol 65(6):277–283. https://doi.org/10.2323/jgam.2018.12.002
33 Xie Z, Thompson A, Kashleva H, Dongari-Bagtzoglou A (2011) A quantitative real-time RT-PCR assay for mature C albicans biofilms. BMC Microbiol 11:93. https://doi.org/10.1186/1471-2180-11-93
34. Hisajima T, Maruyama N, Tanabe Y et al (2008) Protective effects of farnesol against oral candidiasis in mice. Microbiol Immunol 52(7):327–333. https://doi.org/10.1111/j.1348-0421.2008.00044.x
35 Naglik JR, Fidel PL Jr, Odds FC (2008) Animal models of mucosal Candida infection. FEMS Microbiol Lett 283(2):129–139. https://doi.org/10.1111/j.1574-6968.2008.01160.x
36 Yano J, Fidel PL Jr (2011) Protocols for vaginal inoculation and sample collection in the experimental mouse model of Candida vaginitis. J Vis Exp 58:3382. https://doi.org/10.3791/3382